Closing the door on the “puzzle of decoherence” of annihilation quanta

Parashari, Siddharth; Bosnar, Damir; Friščić, Ivica; Kožuljević, Ana Marija; Kuncic, Zdenka; Žugec, Petar; Makek, Mihael

Source / Izvornik: **Physics Letters B, 2024, 852**

Journal article, Published version
Rad u časopisu, Objavljena verzija rada (izdavačev PDF)

https://doi.org/10.1016/j.physletb.2024.138628

Permanent link / Trajna poveznica: https://urn.nsk.hr/urn:nbn:hr:217:945506

Rights / Prava: Attribution 4.0 International/Imenovanje 4.0 međunarodna

Download date / Datum preuzimanja: **2024-11-30**

Repository / Repozitorij:

Repository of the Faculty of Science - University of Zagreb

Phys. Lett. B 852 (2024) 138628

Contents lists available at ScienceDirect

Physics Letters B

journal homepage: www.elsevier.com/locate/physletb

Letter

Closing the door on the "puzzle of decoherence" of annihilation quanta

Siddharth Parashari [a,*], Damir Bosnar [a], Ivica Friščić [a], Ana Marija Kožuljević [a], Zdenka Kuncic [b], Petar Žugec [a], Mihael Makek [a,*]

[a] Department of Physics, Faculty of Science, University of Zagreb, Bijenička c. 32, Zagreb, 10000, Croatia
[b] School of Physics, University of Sydney, Sydney, 2006, New South Wales, Australia

ARTICLE INFO

Editor: B. Blank

Keywords:
Positron annihilation
Quantum entanglement
Decoherence
Gamma polarization
Positron emission tomography
Monte-Carlo simulations

ABSTRACT

In positron annihilation, exploration of the polarization correlations of the emerging gamma quanta has gained interest, since they offer a possibility to improve signal-to-background in medical imaging using positron emission tomography. The annihilation quanta, which are predicted to be in an entangled state, have orthogonal polarizations and this property may be exploited to discriminate them from two uncorrelated gamma photons contributing to the background. Recent experimental studies of polarization correlations of the annihilation quanta after a prior Compton scattering of one of them, had rather different conclusions regarding the strength of the correlation after the scattering, showing its puzzling nature. The scattering was described as a decoherence process. In the present work, we perform for the first time, a study of the polarization correlations of annihilation quanta after decoherence via Compton scattering in the angular range $0° - 50°$ using single-layer gamma ray polarimeters. In addition, we compare the measured polarization correlations after Compton scattering at 30° with an active and a passive scatterer element. The measured azimuthal correlation of back-to-back annihilation quanta is consistent with the Pryce-Ward formulation, as confirmed by Monte Carlo simulations. Further, the results indicate that the correlation, expressed in terms of the polarimetric modulation factor, shows no significant difference at small scattering angles ($0° - 30°$) compared to the correlation measured for direct photons, while a moderate indication of a lower modulation is observed for 50° scattering angle. The measured modulation is larger at all scattering angles than the one expected from the simulation of orthogonally polarized, independent annihilation quanta.

1. Introduction

The correlation of gamma photons emerging from a positron annihilation process has recently become an increasingly interesting research topic with a potential to bring substantial innovations to medical imaging with Positron Emission Tomography (PET) [1–5]. In positron annihilation resulting in two back-to-back γ quanta of 511 keV, they are produced with orthogonal polarizations and are predicted to be in an entangled state. This state can be described by the so called Bell state wave function $|\psi\rangle = (|X\rangle_- |Y\rangle_+ - |Y\rangle_- |X\rangle_+)/\sqrt{2}$, where, $|X\rangle_{+,-}$ and $|Y\rangle_{+,-}$ represent a quantum polarized in (X,Y) propagating in (+,-) $\hat{z}$ direction [10,11,6,7]. The measurement of correlations of annihilation quanta has a long history in physics, starting from the experimental scheme proposed by J. Wheeler [8] to test the predicted correlation of the polarizations of the annihilation photons, where the azimuthal angle difference ($\Delta\phi$) between the scattering planes in double Compton scattering process should have maxima and minima at 90° and 0°, respectively. Similar behavior is also predicted by Pryce and Ward [9] and Snyder et al. [6] by employing the Klein-Nishina approach [12], where the cross-section of a double Compton scattering process is given by [7,9],

$$\frac{d^2\sigma}{d\Omega_1 d\Omega_2} = \frac{r_0^4}{16}\left[F(\theta_1)F(\theta_2) - G(\theta_1)G(\theta_2)\cos(2\Delta\phi)\right] \quad (1)$$

with r_0 being the classical electron radius, $d\Omega_{1,2}$ are the solid angles, $\theta_{1,2}$ are the Compton scattering angles, $\Delta\phi = (\phi_1 - \phi_2)$ is the azimuthal scattering angle difference of gamma particle 1 and 2, respectively. $F(\theta_{1,2}) = \frac{2+(1-\cos\theta_{1,2})^3}{(2-\cos\theta_{1,2})^3}$ and $G(\theta_{1,2}) = \frac{\sin^2\theta_{1,2}}{(2-\cos\theta_{1,2})^2}$ are kinematic factors. The ratio,

* Corresponding authors.
E-mail addresses: siddharth@phy.hr (S. Parashari), bosnar@phy.hr (D. Bosnar), ifriscic@phy.hr (I. Friščić), amk@phy.hr (A.M. Kožuljević), zdenka.kuncic@sydney.edu.au (Z. Kuncic), pzugec@phy.hr (P. Žugec), makek@phy.hr (M. Makek).

https://doi.org/10.1016/j.physletb.2024.138628
Received 9 May 2023; Received in revised form 29 March 2024; Accepted 1 April 2024
Available online 5 April 2024
0370-2693/© 2024 The Author(s). Published by Elsevier B.V. Funded by SCOAP³. This is an open access article under the CC BY license (http://creativecommons.org/licenses/by/4.0/).

$$A(\theta) = \frac{N(\theta, \phi = 90°) - N(\theta, \phi = 0°)}{N(\theta, \phi = 90°) + N(\theta, \phi = 0°)} \quad (2)$$

defines the analyzing power of the polarimeter [13], where $N(\theta, \phi)$ is the number of incoming photons measured at scattering angle θ and azimuthal angle ϕ. The product of the analyzing powers $A(\theta_1)$ and $A(\theta_2)$ is known as the modulation factor (μ) and it measures the polarimetric sensitivity of the detection system. Bohm and Aharonov [10] recognized the azimuthal angle correlation in the double Compton scattering of annihilation photons could be considered an example of entanglement discussed by Einstein, Podolsky, and Rosen [14,15]. Initially, it was shown theoretically that the ratio, $R = (1 + \mu)/(1 - \mu)$ of the scattering probabilities at $\Delta\phi = 90°$ and $\Delta\phi = 0°$, for the wave function in the predicted entangled (separable) state is $R \approx 2.8$ (1.63) [10,6,7,9]. However, the question of evidence of entanglement in Compton scattering of annihilation quanta has been recently readdressed by theoretical works [16,17] and it remains an open topic. The early experiments measured the modulation factors [18–25], among which the most precise measurements were performed by Langhoff [19] and Kasday et al. [22], obtaining $R = 2.47 \pm 0.07$ and $R = 2.33 \pm 0.10$, respectively, which were in good agreement with the predicted value (eq. (1)) considering the finite geometry of the detectors.

Recently, Watts et al. [4] used a simple polarimetric setup based on two Cadmium Zinc Telluride matrices to measure the azimuthal angle correlations of annihilation quanta directly from the source and in another configuration with a passive scatterer. In the latter, a Compton scattering may occur in the path of the photon prior to its detection in the polarimeter. In the measurement of the quanta direct from the source, they obtained a clear modulation of the azimuthal distribution with the measured $R = 1.95 \pm 0.07$ for $\theta_{1,2} = 93° - 103°$. In the configuration with the scatterer positioned at 33° relative to the initial direction, the results indicated the lack of modulation, within the experiment's precision, which they described as a "decohering" process.

In another experiment, Abdurashitov et al. [26,27] used a setup of two gamma-ray polarimeters, each consisting of 16 NaI(Tl) scintillator detectors positioned on a ring, with a plastic scatterer placed at the center. Such geometry enabled precise measurement of the azimuthal angle correlations in events when both annihilation quanta underwent Compton scattering at $\theta_{1,2} = 90°$ yielding the modulation of $R(\mu) = 2.44 \pm 0.02$ (0.418 ± 0.003). In the modified version of the setup, an active scatterer (GAGG scintillator) was placed in front of one plastic scintillator to induce decoherence by Compton scattering one of the photons before entering the polarimeter. The scattered photons then underwent another scattering in the polarimeters yielding the modulation of the azimuthal angle difference of $R(\mu) = 2.41 \pm 0.10$ (0.414 ± 0.017), a result compatible with the one obtained without intentional decoherence.

The results of Abdurashitov et al. [26,27] suggest that the correlation of the azimuthal angles of Compton scattered annihilation quanta is not affected by a prior scattering, at least at small scattering angles $\theta_{scat} \approx 0°$, which disagrees with the finding of Watts et al. [4] suggesting the loss of correlation at $\theta_{scat} \approx 30°$. The clarification of these findings is important on it own merits, but it is also relevant for the implementation of the polarization measurement in PET, where in-silico studies suggested a potential benefit of discriminating the correlated signal events from the uncorrelated background [2].

To resolve the "decoherence puzzle" arising from the previous results, we performed the most comprehensive set of measurements to date. The necessity to resolve this puzzle has also been brought up by Sharma et al., [28]. Our setup based on the single-layer gamma-ray polarimeter concept [3] was able to measure the azimuthal correlation of the annihilation quanta [29,5]. An active scatterer was placed in the path of one annihilation photon to tag the events where that gamma undergoes a prior scattering. One of the detectors could be rotated around the initial direction of the annihilation gamma, enabling the azimuthal correlation measurements at different angles of the prior Compton scattering, θ_{scat}. Thus this setup enabled recreation of the kinematic conditions similar to those in [26,27] ($\theta_{scat} \approx 0°$) and [4] ($\theta_{scat} \approx 30°$), while also significantly extending the explored phase-space to measurements with $\theta_{scat} = 10°$ and $\theta_{scat} = 50°$.

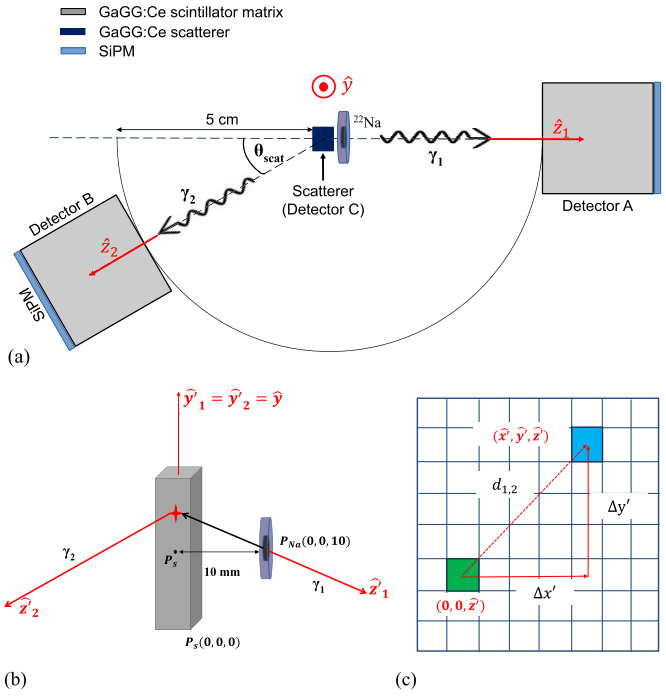

Fig. 1. Schematic diagram of the experimental setup, (a) top view in lab frame, (b) vectors indicating γ_1 and γ_2 propagation direction ($\hat{z}'_{1,2}$) and $\hat{y}'$-axis used to define each gamma's reference frame, P_s and P_{Na} are the coordinates of the scatterer center and ^{22}Na source, respectively, and (c) definition of the azimuthal angles $\phi_{1,2}$ (eq. (3)) from relative positions of the fired pixels in gamma's reference frame.

2. Methodology

2.1. Experimental setup

The experimental setup consists of two single-layer gamma polarimeters [5], denoted as Detector A and B and a scatterer scintillator, denoted Detector C as shown in Fig. 1(a). Each polarimeter encompasses 8×8 GAGG:Ce scintillator matrix with crystal dimensions $1.9 \times 1.9 \times 20$ mm^3 and 2.2 mm pitch. The matrix is read out on one end by a silicon-photomultiplier (SiPM) array, with one-to-one match of crystals and SiPMs. The mean energy resolution (FWHM) of the GAGG:Ce detectors was $8.1 \pm 0.5\%$ at 511 keV. The scatterer (Detector C) was a single scintillating crystal of GAGG:Ce of $3.0 \times 3.0 \times 20$ mm^3 wrapped with teflon. It was read out by one SiPM of a 8x8 SiPM array (KETEK PA3325) and its energy resolution was $12.1 \pm 0.3\%$ at 511 keV. The experiment was performed in the temperature controlled environment keeping the temperature of the Detectors A and B at $18 \pm 1\,°C$. The temperature of the scatterer was further reduced to $15 \pm 1\,°C$ by a Peltier-based cooling system, to improve the sensitivity for low energy events. The data were acquired using the data acquisition and processing system TOFPET2 [30,31]. A modified set of ASIC parameters together with a lower value of time and energy thresholds were used for the data acquisition to enable the acquisition of events with low energy deposits. To do so, the trigger threshold parameters were tuned globally to lower the baseline for dark count rejection and enable trigger for low energy events. The energy measured in each pixel was corrected for SiPM saturation and calibrated using the 511 keV photo-peak from the direct γ-rays. The calibration was independently checked with the 32 keV and 662 keV peaks of ^{137}Cs and was found to be consistent to the level of $\leq 1\%$.

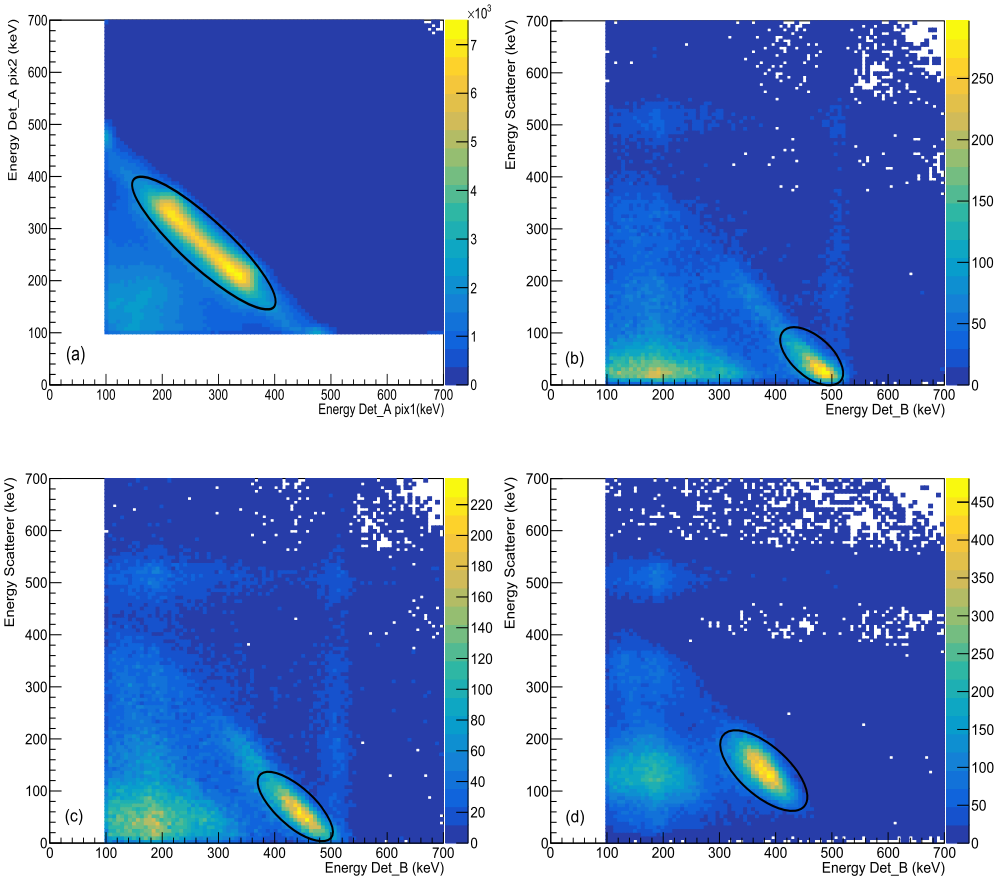

Fig. 2. Energy correlation between two pixels fired in a Compton event in Detector A **(a)**, energy correlation between Detector B and the scatterer Detector C at $\theta_{scat} = 10°$ **(b)**, at $\theta_{scat} = 30°$ **(c)**, and at $\theta_{scat} = 50°$ **(d)**. The selected events are shown with an ellipse.

In the experiment, Detector A was detecting the $\gamma-$ray coming directly from the annihilation event (denoted γ_1), while Detector B was detecting the γ_2 after scattering in the Detector C (the scatterer), which was introduced to induce decoherence by Compton scattering the annihilation photon and to tag such events. Detectors A and B were kept at a fixed distance of 5 cm from the scatterer. Their angular coverage was $\pm 10.1°$ in this geometry. A ^{22}Na-source (1 mm diam., activity $\approx$ 370 kBq, enclosed in 5 mm thick plastic disk) was placed 10 mm from the scatterer between the scatterer and Detector A. Since the expected mean positron range is ≈ 0.5 mm, we assume a vast majority of annihilations occur in close proximity of the source. The events were recorded with Detector B placed at different mean scattering angles, θ_{scat}, of 0°, 10°, 30°, and 50°, while the Detector A was fixed. An additional measurement was performed with Detector B at 30°, in which the scatterer was made passive by being switched off, so it would not contribute to trigger or data acquisition. Such measurement is easily comparable to the one reported by [4], although we note a difference in scatterer geometry.

2.2. Simulations using GEANT4

The experimental scheme shown in Fig. 1 is simulated under the GEANT4 Monte Carlo simulation package version-10.06.p03 [33]. The physics list includes the *G4EmLivermorePolarizedPhysics* and *G4RadioactiveDecayPhysics* models. The simulated geometry includes active volumes of the crystals in both detectors and GAGG scatterer, an isotropic ^{22}Na source (dia. 1 mm, thickness 1 mm), encapsulated in PMMA (5 mm thick). The crystals are placed inside the detector housing filled with epoxy with a silicon photomultiplier attached at the back of each module to keep the simulated geometry and materials as close to the laboratory experiment as possible. The energies registered inside the crystals are smeared with the experimental energy resolutions of the detectors.

Two scenarios are simulated, one with the basic GEANT4 physics models (basic G4-V10) simulating the "classical limit" in which two back-to-back (independent) gammas with orthogonal polarization are generated and another where we implement the Pryce-Ward formulation [9] for the propagation of the Compton scattered annihilation quanta via a so-called *"FastModel"*. The details of the *FastModel* will be separately published elsewhere. The same analysis procedure was followed for the simulated and the experimental data.

2.3. Event selection

Data acquisition was triggered by coincidence events in Detector A and either of Detectors B or C ($A \cap (B \cup C)$). Further event selection was done in the analysis. To select the Compton events that occur in Detectors A or B we required the event to have a multiplicity of 2 fired pixels in the module, where a lower bound of 100 keV was applied to count a pixel as fired to avoid possible noise and cross-talk events. For Detector A, the events where two pixels fired were additionally filtered by requiring the sum of energies of the two fired pixels within 511 ± 70 keV, which corresponds to 3σ around the peak value, and to obey the Compton scattering kinematics. The resulting selection is shown by the outlined region in Fig. 2 (a). To select the annihilation photons that underwent Compton scattering in Detector C and a subsequent Compton scattering following the full absorption in Detector B we required the sum of energies of two fired pixels in Detector B with Detector C are within $511 \pm 3\sigma$ keV. However different types of scattering events can satisfy this condition, which is why we additionally filtered those events that obey the Compton kinematics for scattering at a given θ_{scat}. The

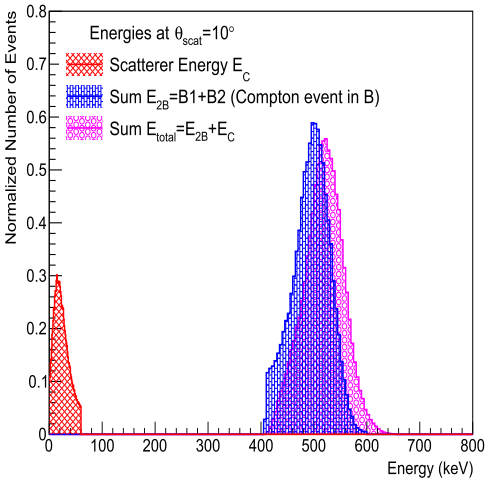

Fig. 3. Energies shared among scatterer and two pixels of Detector B for $\theta_{scat} = 10°$. The total sum of energies adds up to 511 keV.

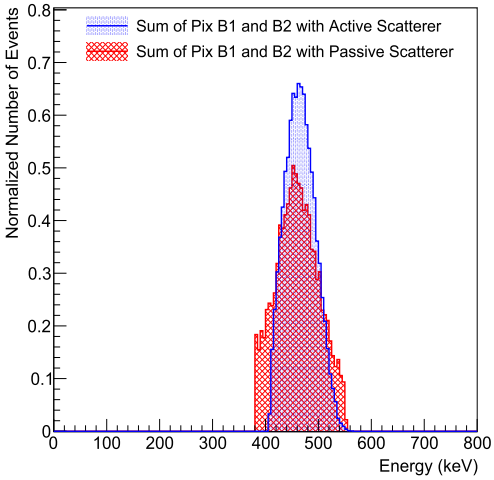

Fig. 4. The sum of energies of two pixels fired in Detector B, for the selected Compton events at $\theta_{scat} = 30°$, active (blue) and passive scatterer (red), using their respective selection criteria.

correlation of energies between Detector C and Detector B under different scattering angles (θ_{scat}) is shown in Fig. 2 (b)-(d), which clearly demonstrates that the energy deposition in Detector C increases with the increasing θ_{scat}, as expected according to Compton kinematics. An example of the energy share of γ_2 in pixels selected for $\theta_{scat} = 10°$ is shown in Fig. 3.

A correlation-baseline measurement (without intentional decoherence), at $\theta_{scat} = 0°$, was performed by selecting events where Detector C did not fire and both energy deposits in Detectors A and B were within $511 \pm 3\sigma$ keV.

An additional measurement was done with the passive scatterer, where the bias voltage of Detector C was switched off. In that case, event selection was done solely based on data from Detectors A and B. The angle of Detector B was set to $\theta_{scat} = 30°$ and its distance from the scatterer was increased to 7.5 cm to avoid direct coincidences between Detectors A and B. In this case, Detector B had an angular coverage of $\pm 6.8°$. Although direct coincidences were avoided by the setup geometry, random coincidences of two annihilation photons from different events could contribute to the expected kinematic region. To avoid such unwanted events we additionally selected true coincidences based on their coincidence time. Hence, the events in which triggering time difference of the corresponding pixels in Detectors A and B was, $\Delta t = |t_1 - t_2| < 1.95$ ns, were selected corresponding to $\pm 3\sigma$ cut on the coincidence time peak. The energy of the selected Compton events in Detector B for $\theta_{\mathrm{scat}} = 30°$ is shown in Fig. 4 and is consistent with the energy spectrum of such events obtained with the active scatterer.

2.4. Determination of azimuthal correlations

For the events where both gammas underwent Compton scattering in Detectors A and B according to the conditions above, we deduce the Compton scattering angle (θ) and the azimuthal angle (ϕ) in each module as:

$$\theta = \mathrm{acos}\left(\frac{\mathrm{m_e c^2}}{\mathrm{E_{px_1} + E_{px_2}}} - \frac{\mathrm{m_e c^2}}{\mathrm{E_{px_2}}} + 1\right); \phi = \mathrm{atan}\left(\frac{\Delta \mathrm{y'}}{\Delta \mathrm{x'}}\right) \quad (3)$$

Due to the ambiguity in the determination of the first and second pixels fired in Compton scattering, by the recoil electron and the scattered gamma, respectively, we have to assume that the first interaction (absorption of the recoil electron) occurs in the pixel with the lower energy deposit ($\mathrm{E_{px_1}} = \mathrm{E_{e'}}$, $\mathrm{E_{px_2}} = \mathrm{E_{\gamma'}}$) since the cross-section and the detector configuration favor forward scattering. According to simulations, for 511 keV gammas scattering at angles $70° < \theta_{1,2} < 90°$, this is true in approximately 52% of events [29]. This ambiguity does not play a significant role in the determination of $\Delta\phi = \phi_1 - \phi_2$, however it contributes to a systematic uncertainty of the modulation factor up to 6.9%.

To reconstruct the $\Delta\phi = \phi_1 - \phi_2$, we adopt the approach to determine the reference frame on event-by-event basis. In each event we first determine the propagation vectors of γ_1 and γ_2, based on the known position of the source and the impact point on detector in laboratory frame (see Fig. 1(b)). These vectors determine the $\hat{z'}_1$, $\hat{z'}_2$ axes of their respective coordinate systems. Since the rotation of Detector B is always in-plane, we choose a common y-axis ($\hat{y'}_1 = \hat{y'}_2 = \hat{y}$). Once the reference frame of each gamma is determined, we transform the measured coordinates in the laboratory frame ($\mathrm{x_{1,2}}, \mathrm{y_{1,2}}, \mathrm{z_{1,2}}$) to coordinates in each gamma's own frame ($\mathrm{x'_{1,2}}, \mathrm{y'_{1,2}}, \mathrm{z'_{1,2}}$) from which we determine the $\phi_{1,2}$ angles according to Eq. (3) as depicted in Fig. 1(c).

For the events that satisfy the Compton selection criteria and for a given range of the reconstructed angles $\theta_{1,2}$, we obtained the distribution of the azimuthal angle differences, $\mathrm{N}(\phi_1 - \phi_2)$, where $\phi_{1,2}$ are the azimuthal angles of the Compton events in Detector A and B, respectively. The $\mathrm{N}(\phi_1 - \phi_2)$ distributions were then corrected for detector acceptance as: $\mathrm{N_{cor}}(\phi_1 - \phi_2) = \mathrm{N}(\phi_1 - \phi_2)/\mathrm{N_{mixed}}(\phi_1 - \phi_2)$. The N_{mixed} is the acceptance determined by event-mixing technique [3,5], where $(\phi_1 - \phi_2)$ is obtained by taking ϕ_1 and ϕ_2 from different randomly chosen events. For each selected Compton event in Detector A, 10^2 random uncorrelated events are sampled in Detector B.

The modulation factor, μ, is determined by fitting the acceptance-corrected distribution, $\mathrm{N_{cor}}(\phi_1 - \phi_2)$, with

$$\mathrm{N_{cor}}(\phi_1 - \phi_2) = \mathrm{M}[1 - \mu \cos(2(\phi_1 - \phi_2))] \quad (4)$$

where M corresponds to the average amplitude of the distribution.

The systematic uncertainty of the determined modulation factor reflects the uncertainty in the determination of $\theta_{1,2}$ angles, resulting from the finite energy resolution of the pixels. We found this contribution to the systematic uncertainty to be 5.8% following the uncertainty of $\sigma_\theta = 6.5°$. The σ_θ broadens the nominally selected $\theta_{1,2}$ window by $\theta_{1,2} \pm \sigma_{\theta_{1,2}}$ and underestimates μ around the maximum value that is achieved for $\theta_{1,2} = 82°$ [5]. Another contribution to the systematic uncertainty of μ comes from the ambiguity in determination of the first and the second pixels fired in Compton scattering. It can be estimated from measured data with no prior scattering, where one can identify and discard events that do not satisfy the back-to-back condition (relative angle $< 165°$). We estimate this contributes up to 6.9% to the systematic uncertainty.

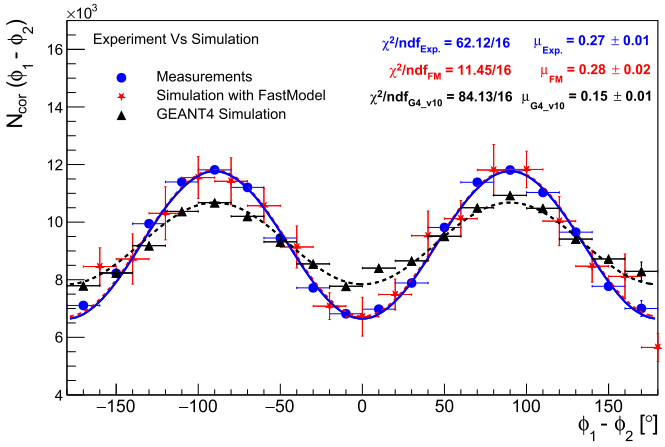

Fig. 5. A comparison between the measurement and simulations for direct (back-to-back) quanta with $72° < \theta_{1,2} < 90°$ and $d_{1,2} > 2.3$ mm. The distributions are fitted with the eq. (4), blue solid curve for experimental data, red dotted for simulation with FastModel, and black dashed for simulation with the basic GEANT4.

3. Results and discussion

To establish the base-line, we measured the azimuthal angle difference for the back-to-back annihilation quanta emerging from positron annihilation without any prior scattering. This setup was also simulated as described in 2.2 in the "classical limit" and with the *Fast Model* implementing the Pryce-Ward formalism. The comparison of the simulation results with the experimental data is shown in Fig. 5. The simulation results of the standard GEANT4 Physics models, establishing the classical limit of the azimuthal modulation for the polarimeters used are inconsistent with the experimentally observed modulation, while simulation with the *Fast Model* is in excellent agreement with the experimentally observed modulation.

The modulation of the azimuthal angle difference was also measured for cases where γ_2 was made decoherent following Compton scattering in the scatterer at $\theta_{\text{scat}} = 0°$, 10°, 30°, and 50°. For quanta of 511 keV, the maximum theoretical modulation ($\mu = 0.48$) is expected for $\theta_{1,2} \approx 82°$ [6,7,9], therefore, for $\theta_{scat} = 0°$, we selected the angular range of $72° < \theta_{1,2} < 90°$. For scattering at $\theta_{\text{scat}} = 30°$ and $\theta_{\text{scat}} = 50°$ the selected angular range in detector B was $73° < \theta_2 < 90°$ and $74° < \theta_2 < 90°$, respectively. This is because the analyzing power $A(\theta) = \sin^2\theta/(\epsilon + 1/\epsilon - \sin^2\theta)$ (derived from eq. (2)) [13] depends on incident to scattered energy ratio, ϵ. Therefore, the maximum analyzing power for $E_2 = 450$ keV (after scattering at $\theta_{\text{scat}} = 30°$) is achieved at $\theta_2 \approx 83°$ yielding the maximum theoretical modulation of $\mu = 0.51$. The maximum analyzing power for $E_2 = 376$ keV (after scattering at $\theta_{\text{scat}} = 50°$) is achieved at $\theta_2 \approx 84°$, predicting the maximum theoretical modulation of $\mu = 0.54$.

The acceptance-corrected distributions of the azimuthal angle differences, $N_{\text{cor}}(\phi_1 - \phi_2)$, for $\theta_{\text{scat}} = 0°$, 10°, 30°, and 50° are shown in Fig. 6. The distribution for the direct measurement (Fig. 6 (a)) exhibits the expected behavior, with the maxima at ±90° indicating the initial orthogonality in the polarizations of the annihilation γs. Similar behavior can be observed in the distributions obtained after Compton scattering by an active scatter (Fig. 6 (b)-(e)) and the passive scatterer (Fig. 6 (f)). The extracted modulation factors listed in Table 1, suggest that the strength of the modulation is largely preserved at all measured scattering angles θ_{scat}, within the precision of the experiment. Such a conclusion seems to be in line with the recent findings of Abdurashitov et al. [26,27] for $\theta_{\text{scat}} = 0°$, additionally extending it up to $\theta_{\text{scat}} = 30°$. Moreover, the azimuthal angle modulation is observed at $\theta_{\text{scat}} = 30°$ with a passive scatterer, even though it was not evident from the measurements by Watts et al. [4].

Table 1
Polarimetric modulation factor, μ, for all measured configurations. Only statistical uncertainties are quoted. The data acquisition time $T_{acq.}$ in each setup is listed.

θ°_{scat}	$\mu \pm \Delta\mu_{stat.}$		$T_{acq.}(hour)$
0°	0.27 ± 0.01*	(0.42 ± 0.12)**	48
10°	0.28 ± 0.03		256
30°	0.30 ± 0.03	$(0.25 \pm 0.05)^{\dagger}$	205 (92)†
50°	0.22 ± 0.06		190

* Direct back-to-back gammas.
** Scattered around $\theta_{scat} = 0°$.
† With the passive scatterer at $\theta_{scat} = 30°$.

If the azimuthal correlation would be completely preserved after the prior Compton scattering, the maximum theoretical modulation factors for scattering at 30° and 50° are 0.505 and 0.538, respectively, while $\mu = 0.48$ is the maximum for the back-to-back case. Experimentally, the measured modulation factor is lower due to the acceptance and resolution of the detectors, which has been confirmed by the conducted simulation for the back-to-back case. In that case the ratio of the measured to ideal modulation is $0.27/0.48 = 0.56$. If we assume this scaling, being a detector property, is valid for other scattering angles, we would expect to measure $\mu = 0.28$ at 30°. This is what we observe (Table 1), within the experimental precision. At $\theta_{\text{scat}} = 50°$, we would expect $\mu = 0.30$, however, we observe an indication of lower modulation, $\mu = 0.22 \pm 0.06$, which may be a hint of a partial depolarization of γ_2, expected for larger scattering angles [34], although firmer conclusions are limited by the statistical precision.

To constrain the possible effects of the experimental apparatus, in addition to the simulation of the back-to-back case, we performed the Geant4 simulation of the scatter setup at $\theta_{\text{scat}} = 30°$ and $\theta_{\text{scat}} = 50°$, simulating the "classical limit", i.e. the positrons from the source annihilating to two orthogonally polarized independent annihilation quanta. We obtain $\mu = 0.14 \pm 0.03$ and $\mu = 0.09 \pm 0.04$, respectively. This is shown in Fig. 6, panels (d) and (f), demonstrating that the modulation expected in this scenario remains significantly lower compared to the measured data.

4. Conclusions

We measured the azimuthal correlations of the back-to-back gamma quanta emerging from positron annihilation, based on their Compton scattering in the single-layer gamma-ray polarimeters. Comparison of the base-line measurements of back-to-back quanta establishes their consistence with the Monte Carlo simulation implementing Pryce-Ward formula, given the detector acceptance and resolution. Measurements were also performed with one of the quanta undergoing a Compton scattering as a decohering process prior to entering the polarimeter and they are compared with the baseline measurement where the annihilation quanta are detected directly from the source. The results show that the strength of the correlation reflected in the measured polarimetric modulation factor does not significantly differ for the case of direct quanta or the case of decoherent quanta for $\theta_{scat} = 0°$, 10°, and 30°. This conclusion differs from indications obtained by Watts et al. [4] for $\theta_{scat} \approx 30°$, but it is in line with the results of Abdurashitov et al. [26,27] for $\theta_{scat} \approx 0°$. For $\theta_{scat} = 50°$, we observe an indication of lower modulation compared to smaller scattering angles, however firm conclusions are limited by the statistical precision. For PET this implies that the polarization correlations cannot discriminate true and scatter coincidences at low angles, however they still may be used for random coincidence rejection.

In conclusion, the measured correlations of annihilation quanta show an interesting behavior that is explored in the broadest kinematic range yet. The experimental results show that their correlations remain strong even after one of them is scattered. Compared to the simula-

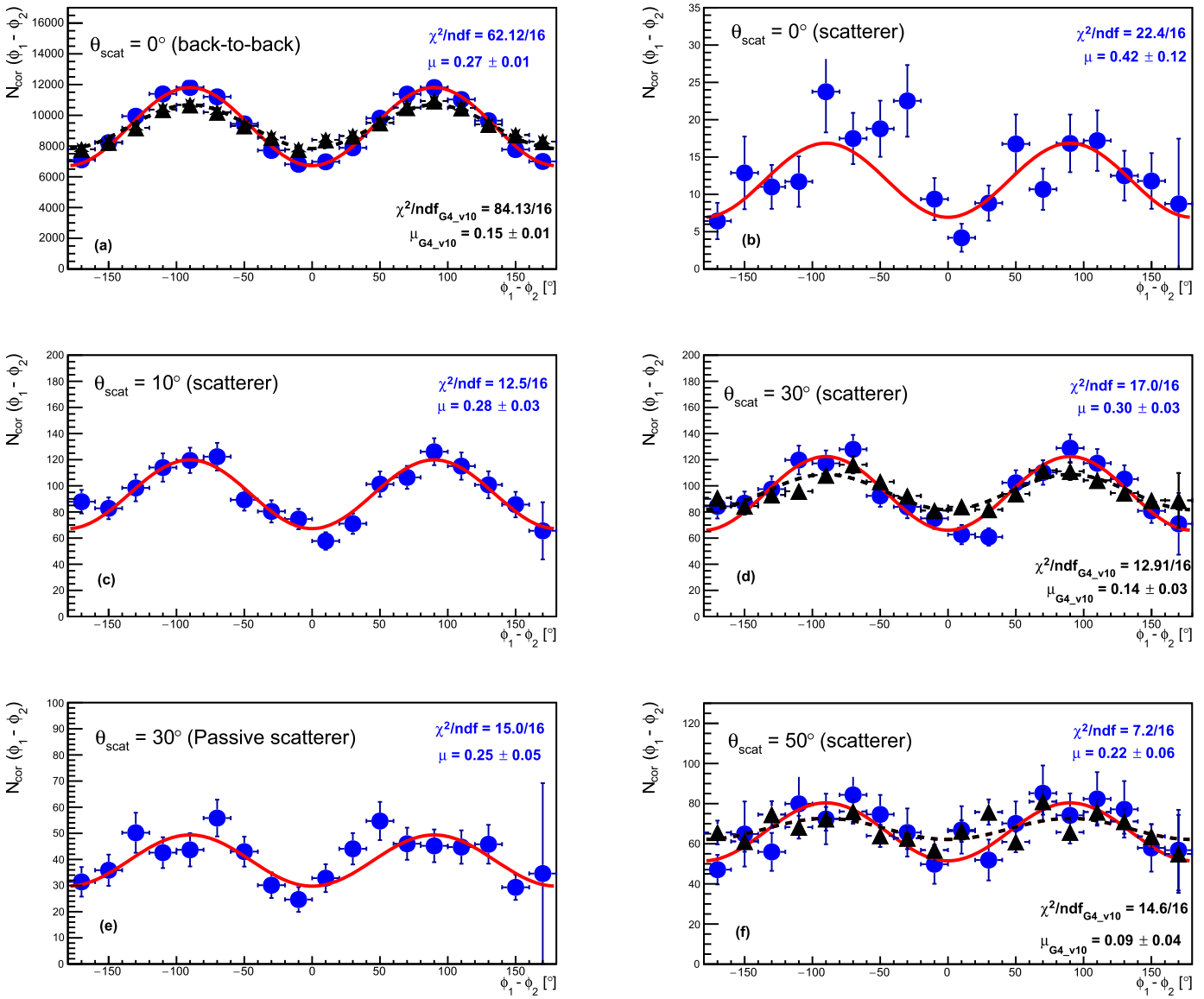

Fig. 6. Azimuthal angle difference distributions for **(a)** direct gammas from the source, with scatterer **(b)** $\theta_{scat} = 0°$, **(c)** $\theta_{scat} = 10°$, **(d)** $\theta_{scat} = 30°$, **(f)** $\theta_{scat} = 50°$, and **(e)** $\theta_{scat} = 30°$ with passive scatterer, respectively. The blue points are the experimental data fit with eq. (4) (red line) to calculate μ. The black triangles represent the Geant4 simulation of the "Classical limit" (dashed line being the fit) for the respective setups in panels **(a)**, **(d)** and **(f)**. The range of Compton scattering angles, $\theta_{1,2}$, in each plot was selected to target maximum expected modulation (see section 3). The uncertainties on μ are scaled by $\sqrt{\chi^2/\text{ndf}}$, in cases where $\chi^2/\text{ndf} > 1$ following recommended error treatment by the Particle Data Group [32].

tion of the independent orthogonally polarized photons, the measured modulation factors remain approximately a factor of two larger at all examined scattering angles.

Declaration of competing interest

The authors declare that they have no known competing financial interests or personal relationships that could have appeared to influence the work reported in this paper.

Data availability

Data will be made available on request.

Acknowledgements

This work was supported in part by the "Research Cooperability" Program of the Croatian Science Foundation, funded by the European Union from the European Social Fund under the Operational Programme Efficient Human Resources 2014–2020, grant number PZS-2019-02-5829, in part by QuantiXLie Center of Excellence, a project co-financed by the Croatian Government and European Union through the European Regional Development Fund — the Competitiveness and Cohesion Operational Programme, grant No. KK.01.1.1.01.0004, in part by EU Horizon 2020 research and innovation programme under project OPSVIO, Grant Agreement No. 101038099 and in part by Croatian Science Foundation under the project IP-2022-10-3878. The authors acknowledge support of Laboratory for Advanced Computing at the Department of Physics, Faculty of Science University of Zagreb in running GEANT4 simulations.

References

[1] A. McNamara, et al., Towards optimal imaging with PET: an in silico feasibility study, Phys. Med. Biol. 59 (2014) 7587, https://doi.org/10.1088/0031-9155/59/24/7587.

[2] M. Toghyani, et al., Polarisation-based coincidence event discrimination: an in silico study towards a feasible scheme for Compton-PET, Phys. Med. Biol. 61 (2016) 5803, https://doi.org/10.1088/0031-9155/61/15/5803.
[3] M. Makek, et al., Single-layer Compton detectors for measurement of polarization correlations of annihilation quanta, Nucl. Instrum. Methods Phys. Res., Sect. A 958 (2020) 162835, https://doi.org/10.1016/j.nima.2019.162835.
[4] D.P. Watts, et al., Photon quantum entanglement in the MeV regime and its application in PET imaging, Nat. Commun. 12 (2021) 2646, https://doi.org/10.1038/s41467-021-22907-5.
[5] S. Parashari, et al., Optimization of detector modules for measuring gamma-ray polarization in Positron Emission Tomography, Nucl. Instrum. Methods Phys. Res., Sect. A 1040 (2022) 167186, https://doi.org/10.1016/j.nima.2022.167186.
[6] H.S. Snyder, S. Pasternack, J. Hornbostel, Angular correlation of scattered annihilation radiation, Phys. Rev. 73 (1948) 440, https://doi.org/10.1103/PhysRev.73.440.
[7] J.C. Ward, Some Properties of Elementary Particles, Ph.D. Thesis, University of Oxford, 1949.
[8] J. Wheeler, Polyelectrons, Ann. N.Y. Acad. Sci. 48 (1946) 219, https://doi.org/10.1111/j.1749-6632.1946.tb31764.x.
[9] M.H.L. Pryce, J.C. Ward, Angular correlation effects with annihilation radiation, Nature 160 (1947) 435, https://doi.org/10.1038/160435a0.
[10] D. Bohm, Y. Aharonov, Discussion of experimental proof for the paradox of Einstein, Rosen, and Podolsky, Phys. Rev. 108 (1957) 1070, https://doi.org/10.1103/PhysRev.108.1070.
[11] S.J. Bell, On the Einstein Podolsky Rosen paradox, Physics 1 (1964) 195, https://doi.org/10.1103/PhysicsPhysiqueFizika.1.195.
[12] O. Klein, T. Nishina, Über die Streuung von Strahlung durch freie Elektronen nach der neuen relativistischen Quantendynamik von Dirac, Z. Phys. 52 (1929) 853, https://doi.org/10.1007/BF01366453.
[13] P. Knights, et al., Studying the effect of polarisation in Compton scattering in the undergraduate laboratory, Eur. J. Phys. 39 (2018) 025203, https://doi.org/10.1088/1361-6404/aa9c98.
[14] A. Einstein, B. Podolsky, N. Rosen, Can quantum-mechanical description of physical reality be considered complete?, Phys. Rev. 47 (1935) 777, https://doi.org/10.1103/PhysRev.47.777.
[15] A. Einstein, Zur Elektrodynamik bewegter Körper (On the electrodynamics of moving bodies), Ann. Phys. 322 (1905) 891, https://doi.org/10.1002/andp.19053221004.
[16] B.C. Hiesmayr, P. Moskal, Witnessing entanglement in Compton scattering processes via mutually unbiased bases, Sci. Rep. 9 (2019) 8166, https://doi.org/10.1038/s41598-019-44570-z.
[17] P. Caradonna, D. Reutens, T. Takahashi, S. Takeda, V. Vegh, Probing entanglement in Compton interactions, J. Phys. Commun. 3 (2019) 105005, https://doi.org/10.1088/2399-6528/ab45db.
[18] C.S. Wu, I. Shaknov, The angular correlation of scattered annihilation radiation, Phys. Rev. 77 (1950) 136, https://doi.org/10.1103/PhysRev.77.136.
[19] H. Langhoff, Die linearpolarisation der vernichtungsstrahlung von positronen, Z. Phys. 160 (1960) 186–193, https://doi.org/10.1007/BF01336980.
[20] L.R. Kasday, in: B. d'Espagnat (Ed.), Foundations of Quantum Mechanics: Proceedings of the International, School of Physics "Enrico Fermi", 1971, pp. 195–210.
[21] G. Faraci, et al., An experimental test of the EPR paradox, Lett. Nuovo Cimento 9 (1974) 607–611, https://doi.org/10.1007/BF02763124.
[22] L.R. Kasday, J.D. Ullman, C.S. Wu, Angular correlation of Compton-scattered annihilation photons and hidden variables, Il Nuovo Cimento B 25B (1975) 633–661, https://doi.org/10.1007/BF02724742.
[23] A. Wilson, J. Lowe, D. Butt, Measurement of the relative planes of polarization of annihilation quanta as a function of separation distance, J. Phys. G, Nucl. Phys. 2 (1976) 613–624, https://doi.org/10.1088/0305-4616/2/9/009.
[24] M. Bruno, M. D'Agostino, C. Maroni, Measurement of linear polarization of positron annihilation photons, Il Nuovo Cimento B 40 (1976) 143–152, https://doi.org/10.1007/BF02739186.
[25] G. Bertolini, E. Diana, A. Scotti, Correlation of annihilation γ-ray polarization, Il Nuovo Cimento B 63 (1981) 651–665, https://doi.org/10.1007/BF02755105.
[26] D. Abdurashitov, et al., Setup of Compton polarimeters for measuring entangled annihilation photons, J. Instrum. 17 (P03010) (2022), https://doi.org/10.1088/1748-0221/17/03/P03010.
[27] A. Ivashkin, et al., Testing entanglement of annihilation photons, Sci. Rep. 13 (2023) 7559.
[28] S. Sharma, D. Kumar, P. Moskal, Decoherence puzzle in measurements of photons originating from electron–positron annihilation, Acta Phys. Pol. 142 (2022) 428, https://doi.org/10.12693/APhysPolA.142.428.
[29] A.M. Kožuljević, et al., Study of multi-pixel scintillator detector configurations for measuring polarized gamma radiation, Condens. Matter 6 (2021) 43, https://doi.org/10.3390/condmat6040043.
[30] A.D. Francesco, et al., TOFPET2: a high-performance ASIC for time and amplitude measurements of SiPM signals in time-of-flight applications, J. Instrum. 11 (2016) C03042.
[31] R. Bugalho, et al., Experimental characterization of the TOFPET2 ASIC, J. Instrum. 14 (P03029) (2019), https://doi.org/10.1088/1748-0221/14/03/P03029.
[32] M. Tanabashi, et al., Review of particle physics, Phys. Rev. D 98 (3) (2018) 030001, https://doi.org/10.1103/PhysRevD.98.030001.
[33] Agostinelli, et al., GEANT4—a simulation toolkit, Nucl. Instrum. Methods Phys. Res., Sect. A, Accel. Spectrom. Detect. Assoc. Equip. 506 (2003) 250.
[34] G.O. Depaola, New Monte Carlo method for Compton and Rayleigh scattering by polarized gamma rays, Nucl. Instrum. Methods Phys. Res., Sect. A 512 (2013) 619–630, https://doi.org/10.1016/S0168-9002(03)02050-3.